

Dual Polarization Synthesis and Optimization of Cylindrical Offset Reflector Antenna for Cosecant-squared Radiation Pattern

R. Vahdani, T. Azad, V. Mohtashami and A. R. Attari

Department of Electrical Engineering, Ferdowsi University of Mashhad, Mashhad, Iran
t_azad_69@yahoo.com@gmail.com, reza.vahdani90@yahoo.com, v.mohtashami@um.ac.ir, attari50@um.ac.ir
Corresponding Author: V. Mohtashami

Abstract- This paper presents the shaping optimization of an S-band cylindrical offset reflector antenna with cosecant-squared radiation pattern in elevation plane. The cross section of the antenna is mathematically modeled by a polynomial function and optimized by the genetic algorithm to obtain the desired pattern for both TE and TM polarizations. The physical optics method together with the uniform theory of diffraction is used to efficiently calculate the radiation pattern during the optimization. Numerical results show that the cosecant-squared radiation pattern can be achieved with good accuracy for angular span of 50^{st} . The computed radiation pattern agrees well with method of moments as well as CST software package and deviates less than about 0.7 dB, on average, from the ideal cosecant-squared pattern.

Index Terms-Cosecant-squared pattern, genetic algorithm, physical optics, reflector antenna, uniform theory of diffraction.

I. INTRODUCTION

Cosecant-squared radiation pattern is usually required by air surveillance radars in order to guarantee constant power reception from a target that flies at a constant altitude [1]. Other applications include ground mapping radars and wireless networks [2]. Various antenna configurations such as Butler matrix [3], microstrip array [4], linear phased array [5] and shaped reflector [6–10] have been suggested to achieve cosecant-squared radiation pattern. Among them, shaped reflector antenna is a good choice due to its simple structure that is straightforward to fabricate and does not need expensive beam-forming networks.

At low microwave frequencies, the size of the reflector is large and its surface roughness is small with respect to the wavelength. Consequently, the Physical Optics (PO) method provides proper accuracy and computational efficiency for the design and analysis of the reflector. When

supplemented by the uniform or physical theory of diffraction, the current distribution is calculated with good accuracy all over the surface and near the edge of the reflector [11]. To facilitate the design

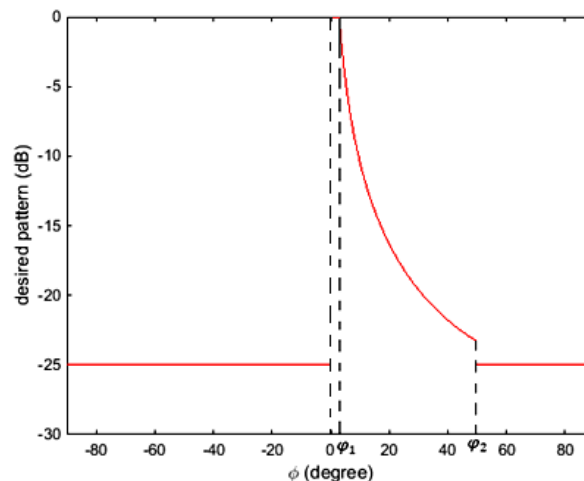


Fig. 1. Desired normalized cosecant-squared radiation pattern.

process, a proper mathematical surface representation should be used. Polynomial function and Fourier-Jacobi expansion are among the reported representations in the literature [6, 12].

This paper presents the synthesis and optimization of a cylindrical offset reflector antenna that produces cosecant-squared radiation pattern in elevation plane at S-band frequencies. This specific problem has practical applications in industry and was referred to the authors. The cross section of the reflector is represented by a polynomial function. To achieve the desired radiation pattern, the coefficients of the polynomial are optimized by using Genetic Algorithm (GA). The design procedure yields cosecant-squared radiation pattern in both TE and TM polarizations. The computational burden and the accuracy of the optimization process are handled by using the physical optics method and Uniform Theory of Diffraction (UTD). Two reference solutions, CST software as well as author-generated code based on the method of moments, are used to validate the simulation results. Then, the radiation pattern of the designed reflector antenna is compared with these reference solutions. It is assumed throughout the text that a conventional feed (such as an open-ended waveguide or a horn antenna) with proper matching has been used to feed the reflector.

The paper is organized as follows. The analysis and design of the antenna as well as shape optimization are described in Section II. Numerical results and discussion are presented in Section III and conclusions are given in section IV.

II. DESIGN AND ANALYSIS

The cosecant-squared radiation pattern of an antenna in the elevation plane over the range of angles $\varphi_1 \leq \varphi \leq \varphi_2$ is

$$G(\varphi) = G_0 \csc^2(\varphi) \quad (1)$$

where G_0 is a constant that depends on the gain of the antenna. Fig. 1 shows the desired normalized

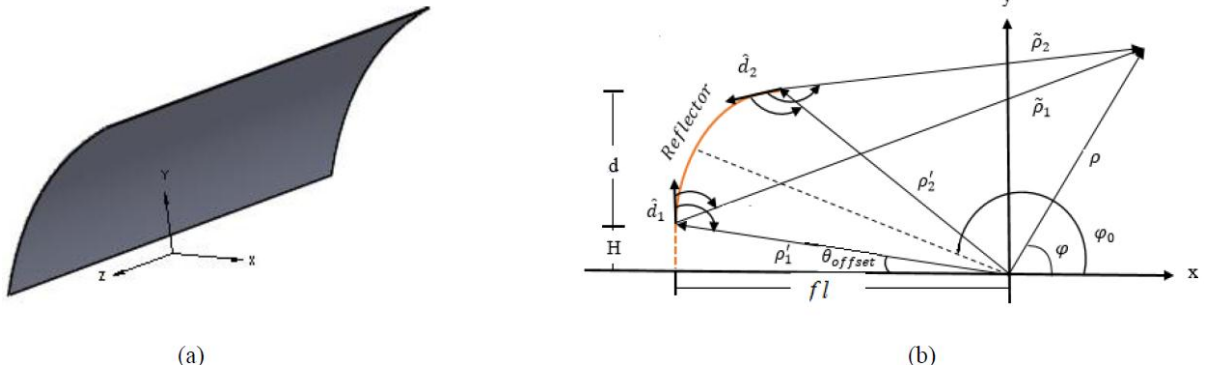


Fig. 2. Geometry of the cylindrical offset reflector antenna, (a) 3D view, (b) cross section.

pattern in the angular span of the elevation plane. The horizon is assumed at $\varphi = 0^\circ$. Ideal cosecant-squared pattern is desired over $\varphi_1 \leq \varphi \leq \varphi_2$ whereas side lobe less than a predefined level (e.g. -25 dB as shown in the figure) is required over $-90^\circ \leq \varphi \leq 0^\circ$ and $\varphi_2 \leq \varphi \leq 90^\circ$. The region $0^\circ \leq \varphi \leq \varphi_1$ is assumed as transition region. Typical values of φ_1 and φ_2 are a few degrees and several tens of degrees respectively. To present the systematic procedure used for design and optimization of the reflector, this section is divided into three subsections. The first subsection describes geometry of the reflector and parameters of the feed. The second subsection formulates the problem by using PO and UTD. The last subsection presents the optimization process and the associated cost function.

A. Antenna Geometry

The geometry of the cylindrical reflector antenna is shown in Fig. 2(a). The reflector is flat along the z -axis and is assumed very long compared to wavelength in that direction. As a result, we deal with a 2-dimensional problem as shown in Fig. 2(b). The cross section of the antenna is shaped to achieve cosecant-squared pattern in the elevation xy plane. Note that the cylindrical reflector is flat along the z -axis and therefore radiates a pencil beam (sinc function) in the azimuth xz plane [13].

The cross section of the offset reflector is represented as

$$x = f(y); \quad H \leq y \leq H + d \quad (2)$$

where d is the aperture size, and $f(y)$ is assumed a polynomial function of the form

$$x = \sum_{n=0}^N a_n y^n \quad (3)$$

Furthermore, H is a positive value that represents the offset of the reflector. It is adjusted to eliminate the blockage of the feed located at the origin of the coordinate system. The polynomial function provides a continuous description of the cross section and facilitates the design process. The coefficients of the polynomial are determined during the optimization process. The polynomial degree is empirically chosen according to the computational burden of the optimization.

B. Formulation

Since the cylindrical reflector is very long along the z -axis direction, a 2-dimensional analysis is applied. The normalized pattern of feed $(S(\varphi'))^2$ is assumed to be of the cosine power form defined by [14]

$$(S(\varphi'))^2 = \begin{cases} \cos^q(\varphi' - \varphi_0) & ; \quad 0 \leq |\varphi' - \varphi_0| \leq \pi/2 \\ 0 & ; \quad \text{else} \end{cases} \quad (4)$$

where q is adjusted to obtain the desired tapering level at edges of the reflector. The feed points to the center of the reflector and the direction of maximum radiation of the feed is denoted as φ_0 . It is also assumed that no power leaks to the back of feed ($\pi/2 \leq |\varphi' - \varphi_0| \leq \pi$). The reflector is located in the far field of the feed and, therefore, the incident field on the reflector surface is a cylindrical wave

$$\psi^i = \psi_0 \frac{e^{-jk\rho'}}{\sqrt{\rho'}} S(\varphi') \quad (5)$$

where ψ^i represents E_z^i and H_z^i in TM^z (soft) and TE^z (hard) polarizations respectively. The value of ψ_0 depends on the gain and radiation power of the feed. Note that primed coordinates are used in (4) because this incident field induces surface current on the reflector and the final scattered field is obtained by integrating over this current.

To calculate the field scattered by the reflector, the physical optics method is used to calculate the induced current density on the illuminated part of the surface. The illuminated part of the reflector is determined by ray tracing intersection test [15]. Then, the scattered field is calculated via the radiation integral [13]

$$\mathbf{H}^s = \int_{S_i} \nabla G(\mathbf{r}, \mathbf{r}') \times \mathbf{J}_s(\mathbf{r}') ds' \quad (6)$$

where S_i is the illuminated part of the surface, $G(\mathbf{r}, \mathbf{r}') = H_0^{(2)}(k|\mathbf{r} - \mathbf{r}'|)/4j$ is the 2-dimensional Green's function and $\mathbf{J}_s(\mathbf{r}') = 2\hat{n}(\mathbf{r}') \times \mathbf{H}^i(\mathbf{r}')$ is the induced current density. By calculating the gradient of the Green's function, applying the principles of vector calculus as well as far-field approximations, the physical optics scattered field ψ^s is analytically derived in the compact form as

$$\psi^s = \sqrt{\frac{k}{2\pi}} e^{-j3\pi/4} \psi_0 P(\varphi) \frac{e^{-jk\rho}}{\sqrt{\rho}} \quad (7)$$

where (ρ, φ) is the cylindrical coordinates of the observation point. The function $P(\varphi)$ is the pattern of the scattered field which is obtained for TM^z polarization as

$$P(\varphi) = \int_H^{H+d} \left[S(\varphi') \frac{e^{-jk\rho'}}{\sqrt{\rho'}} e^{jk(f(y')\cos\varphi + y'\sin\varphi)} \left(-\cos\varphi' + \frac{df}{dy'} \sin\varphi' \right) \right] dy' \quad (8)$$

where $f(y')$ is the polynomial function that describes the reflector geometry. Note that (ρ', φ') are expressed in terms of the integration variable as $\rho' = (y'^2 + [f(y')]^2)^{1/2}$, $\varphi' = \pi + \tan^{-1}(y'/f(y'))$. For TE^z polarization the scattering pattern is obtained as

$$P(\varphi) = \int_H^{H+d} \left[S(\varphi') \frac{e^{-jk\rho'}}{\sqrt{\rho'}} e^{jk(f(y')\cos\varphi + y'\sin\varphi)} \left(-\cos\varphi + \frac{df}{dy'} \sin\varphi \right) \right] dy' \quad (9)$$

which is very similar to (8) except for the prime elimination of φ in the last parentheses. The reason is the direction of the induced current density; it is along the z-axis in TM^z polarization whereas it is in xy plane in TE^z polarization. The integrals can be calculated either by exact numerical techniques such as adaptive quadrature methods, or by approximate techniques such as the method of stationary phase [14].

In order to improve the accuracy of the results, the diffracted fields from the two edges of the reflector have to be added to the physical optics field. The uniform theory of diffraction provides a straightforward and accurate solution. Due to the locality of electromagnetic fields at high frequencies [13], each of the reflector edges can be locally approximated by a half plane whose normal vector is in xy plane and perpendicular on the tangent vector to the reflector at the edge point. The orientations of the two approximate half planes are denoted as \hat{d}_1, \hat{d}_2 in Fig. 2(b). This

way, the diffracted field of the m th edge, denoted as ψ^{d_m} , $m = 1, 2$, is calculated based on the canonical problem of half-plane diffraction as [13]

$$\psi^{d_m} = \psi^i(\rho'_m) D_{UTD} \frac{e^{-jk\rho_m}}{\sqrt{\rho_m}} \quad (10)$$

where ρ'_m and ρ_m are respectively the distances of the m th edge from the feed and the field point. The diffraction coefficient D_{UTD} equals $D_i m D_r$, where D_i is the incident-diffraction coefficient, D_r is the reflection-diffraction coefficient, and the minus and plus signs are used for TM^z and TE^z polarizations respectively [13]. Note that in our problem, the source point (feed) is located at a finite distance from the edge and the diffracted field has to be calculated in far field. This differs from the canonical half-plane diffraction problem in which the plane wave diffracted field is obtained at a finite distance from the edge. Due to reciprocity theorem, however, the diffraction coefficients for our problem can be calculated by swapping the coordinates of the field and source points in the diffraction coefficients of the canonical problem. The total scattered field is the coherent sum of the physical optics field and the diffracted fields from the two edges.

C. Shape Optimization

To achieve the cosecant-squared radiation pattern, the surface of the reflector should be systematically shaped by using an optimization technique. In any optimization process a proper cost function must first be defined that covers the concerns of the designer. Referring to Fig. 1, the radiation pattern must fit the ideal cosecant-squared radiation pattern in angular span $\varphi_1 \leq \varphi \leq \varphi_2$. Furthermore, the radiation pattern must be kept below a predefined side lobe level outside this angular region. Note that the radiation pattern is normalized to its maximum value at φ_1 , and its value in the transition region ($0 \leq \varphi \leq \varphi_1$) is neglected throughout the optimization process. The quality of the design is assessed by analyzing the radiation pattern in logarithmic scale.

The cost function C is defined as

$$C = w_1 \bar{E}_{\text{csc}^2} + w_2 \bar{E}_{\text{sll}} \quad (11)$$

where

$$\bar{E}_{\text{csc}^2} = \frac{1}{L_1} \sum_{i=1}^{L_1} e_1(i) \quad (12)$$

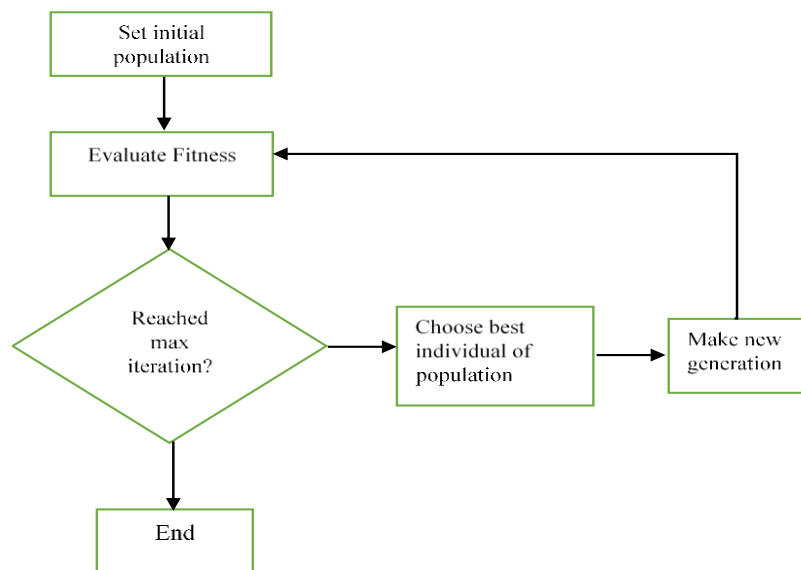
is the average difference between the obtained normalized pattern and the ideal cosecant-squared pattern, and

$$\bar{E}_{sll} = \frac{1}{L_2} \sum_{j=1}^{L_2} e_2(j) \quad (13)$$

is the average cost of exceeding the side lobe level. Specifically, L_1 is the number of sampling points in angular region $\varphi_1 \leq \varphi \leq \varphi_2$ and $e_1(i)$ is the absolute value of the logarithmic difference between the obtained and ideal pattern at i th sampling angle. Furthermore, L_2 is the number of sampling points outside $\varphi_1 \leq \varphi \leq \varphi_2$ and $e_2(j)$ is defined as

$$e_2(j) = \frac{X(j) + |X(j)|}{2} \quad (14)$$

where $X(j)$ is the logarithmic field level in excess of the predefined side lobe level at j th sampling angle. Note that if the field level is less than the predefined side lobe level, $e_2(j)$ will be zero, as expected. In (11), the user-defined coefficients w_1 and w_2 weight the significance of the two mentioned factors in the cost function. In order to design a dual-polarized antenna, the cost function is simultaneously minimized for both TM^z and TE^z polarizations.



The Genetic Algorithm is used as the optimization algorithm. It is an iterative evolutionary search algorithm which converges to the global minimizer of the problem [16]. Fig. 3 shows the flowchart of the optimization procedure. In our current problem the coefficients of the polynomial that define the shape of the reflector are optimized. At each iteration, the generated coefficients are used and the radiation pattern and the cost function are then computed. This

process is repeated until a predefined number of iterations is reached and the shaped reflector with desired pattern is designed. The degree of the polynomial and the number of iterations of the optimization process are selected according to the available computational resources and the desired accuracy. Detailed discussion on the numerical results is presented in the next section.

III. NUMERICAL RESULTS AND DISCUSSION

The reflector is designed to achieve the cosecant-squared radiation pattern. With reference to Fig. 1, the values $\varphi_1 = 3^\circ$, $\varphi_2 = 50^\circ$ and $SLL = -25$ dB are considered for the design procedure. Extending this angular span and/or realizing lower side lobe level only increase the computational burden, but the optimization procedure remains the same. Realizing the cosecant-squared pattern is usually more important and computationally intensive than reducing the side lobe level. As a result, the weighting coefficients of the cost function are selected $w_1 = 2/3$ and $w_2 = 1/3$.

Large dimensions of the reflector are desirable for more radiation gain, but, on the other hand, physical limitations due to weight and volume do not permit very large sizes. Here, the diameter of reflector is selected $d = 3$ m which is 30 times the wavelength at operation frequency of 3 GHz. To ensure blockage elimination, the offset angle is selected a few degrees based on the size of the feed. It

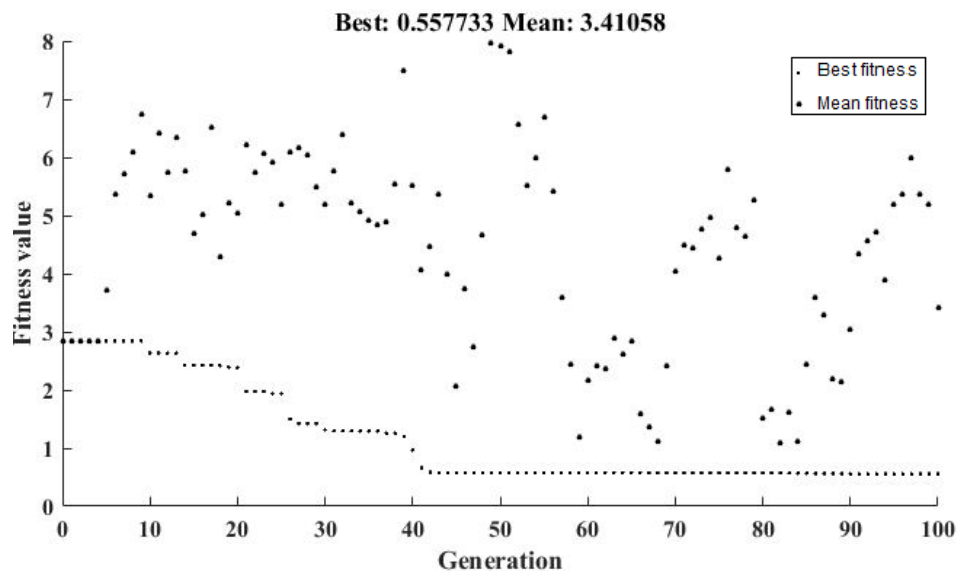


Fig. 4 Convergence curve of the fitness function

is set at $\theta_{\text{offset}} = 5^\circ$ in our simulation assuming that a C-band horn antenna is used as the feed. The initial geometry of the surface is chosen as a cylindrical parabolic reflector. The focal length

is $f_i = 2.5885$ m and the corresponding polynomial coefficients with four-digit precision are given in Table I. The offset parameter is set $H = 0.226$ m based on the selected offset angle and the focal length of the reflector.

The feed points toward the center of the angular region that the initial parabolic reflector occupies. According to the selected values of d , H , f_i , the direction of maximum radiation is computed $\varphi_0 = 145.6^\circ$. The value q in (4) is set 10 which produce -6 dB tapering at the edges of the reflector surface.

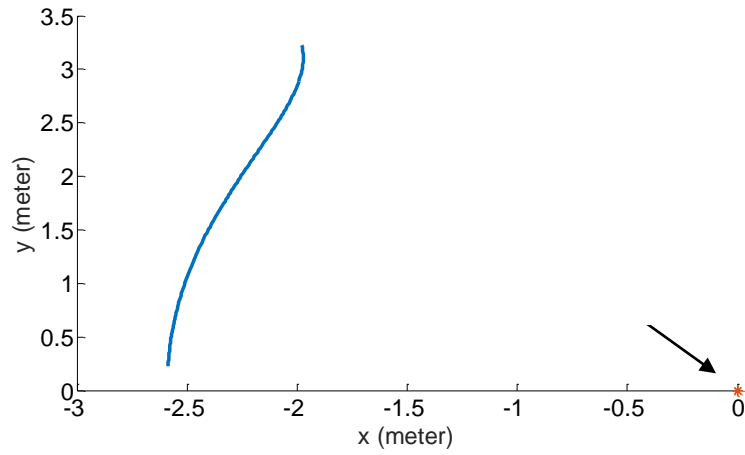
The Genetic Algorithm (GA) is used for optimizing the polynomial coefficients of the reflector surface. Population size of every generation in GA optimization process is empirically selected 10. Lower population sizes have been found unable to provide the optimization goals whereas higher population sizes significantly increase the computational burden with little improvement in the final result. The polynomial degree is selected 6, which is found to provide a good trade-off between the accuracy of the results and the computational burden of the optimization. In order to retain the overall shape of the offset reflector, the value of a_0 is not changed and the optimization procedure involves the rest of the polynomial coefficients. One of the members in the initial population of GA is chosen based on Table I and setting other polynomial coefficients to zero. At each iteration, PO and UTD are used to calculate the radiation pattern in both TM^z and TE^z polarizations. The pattern described by (8), (9) are numerically calculated by using global adaptive quadrature method. The best individual of the population with minimum value of cost function is determined and passed to the next generation. Other members of the next generation are generated by mutation and cross-over operations. This process is repeated until the GA algorithm converges, the cost function is minimized and the desired

Table I. Polynomial coefficients for initial geometry of the reflector.

a_0	a_1	a_2
-2.5885	0	0.0966

Table II. Optimized polynomial coefficients describing the surface of the reflector.

a_0	a_1	a_2	a_3	a_4	a_5	a_6
-2.5885	-0.0101	0.0888	-0.0026	0.0016	0.0012	-0.0007



pattern is achieved. The convergence curve of the fitness function is shown in Fig. 4. As observed, the convergence is achieved after 100 iterations in our simulation.

Table II shows the values of optimized polynomial coefficients. The resulting geometry of the reflector is also depicted in Fig. 5. Note that the antenna is flat along the z -axis and Fig. 5 shows the cross section of the synthesized antenna. The shaped reflector radiates cosecant-squared pattern in the elevation plane as depicted in Fig. 6 for both TM^z and TE^z polarizations.

Two reference solutions, CST software as well as a code based on the method of moments (generated by the authors), are used to validate the simulation results. A snapshot of the geometry simulated by CST is depicted in Fig. 7. The developed code base on the method of moments is the other reference solution to validate the simulation results. Since we are dealing with an open surface, the Electric Field Integral Equation (EFIE) is solved. The surface current density has only z component in TM^z polarization whereas it has both x and y components in TE^z polarization. The point-matching technique is used to discretize the integral equation over the reflector surface with sampling rate of 20 segments per wavelength. The surface current density is obtained by solving the

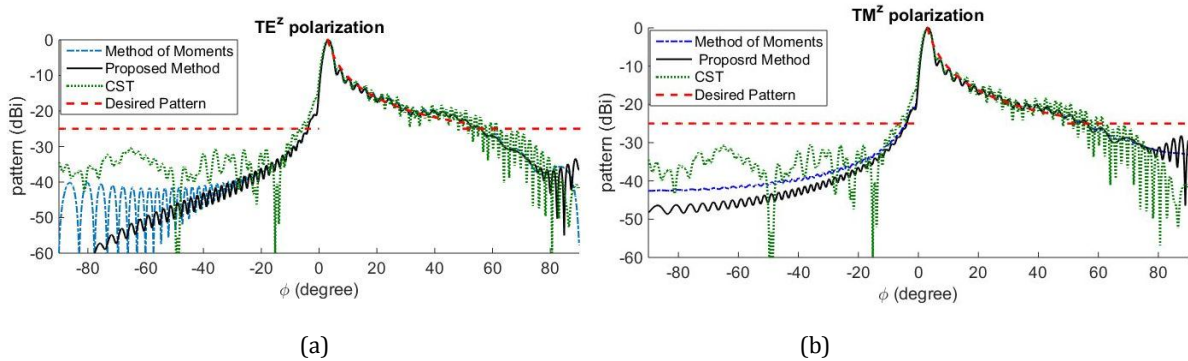


Fig. 6. The radiation pattern of the shaped reflector at 3 GHz, (a) TE^z polarization, (b) TM^z polarization.

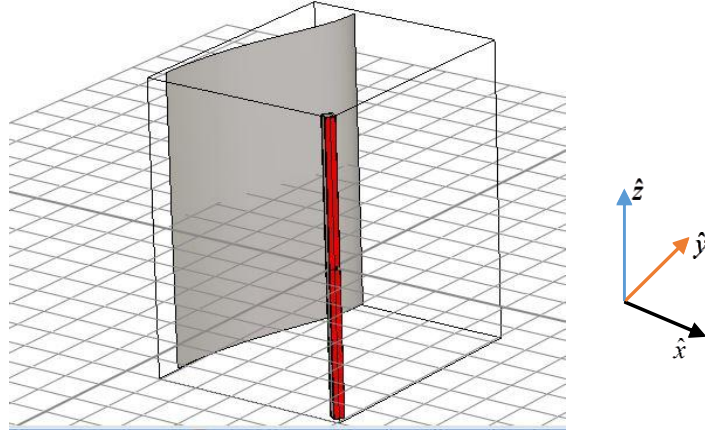


Fig. 7. The geometry of shaped reflector fed by a long open-ended rectangular waveguide in CST environment

Table III. characteristics of the obtained radiation pattern for low, mid and high frequencies

Frequency (GHz)	$\bar{E}_{\text{csc}^2}^{TMz}$	$\bar{E}_{\text{csc}^2}^{TEz}$	$\bar{E}_{\text{sil}}^{TMz}$	$\bar{E}_{\text{sil}}^{TEz}$	$\text{Gain}^{TMz} \text{ (dBi)}$	$\text{Gain}^{TEz} \text{ (dBi)}$
2.5	0.75	0.70	0.33	0.33	34.9	35
3	0.65	0.58	0.18	0.18	36.5	36.6
4	0.97	0.94	0.09	0.06	38.7	38.7

resulting linear equation system. Then, the radiation integral is calculated and the scattered field is obtained. The results of CST and the method of moments are shown in Fig. 6 for validation of the

designed reflector pattern. As observed, the radiation pattern of the designed reflector agrees well with CST and the method of moments in the angular region of interest. This confirms the validity of our field computations and optimization procedure. The CST simulation takes 40 minutes to complete on a personal computer with Intel core i7 4790 4 GHz CPU and 32GB memory, whereas a single run of our physical optics simulation runs instantaneously. Due to the large size of the reflector, the simulation would have been very intensive if the CST simulation were used for field computations

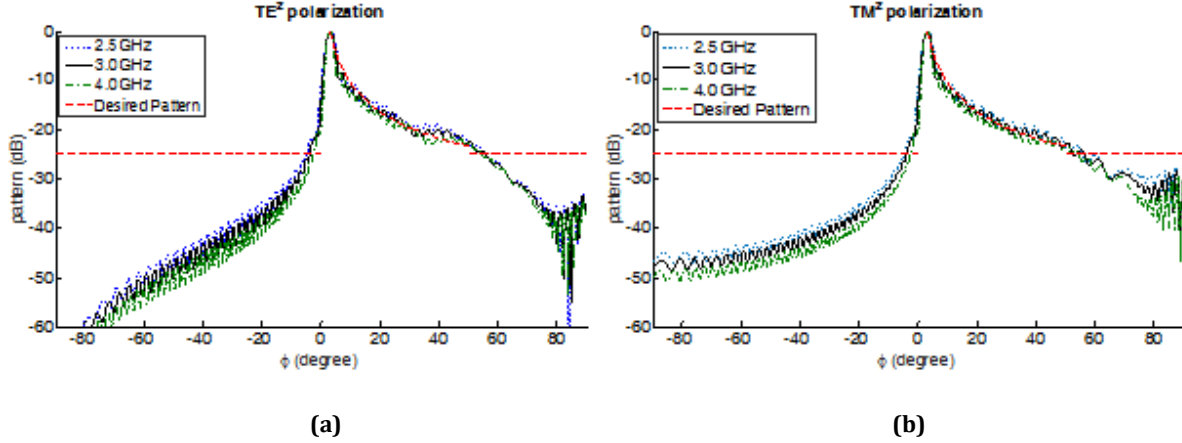


Fig. 8. Frequency variation of radiation pattern in elevation plane, (a) TE^z polarization, (b) TM^z polarization.

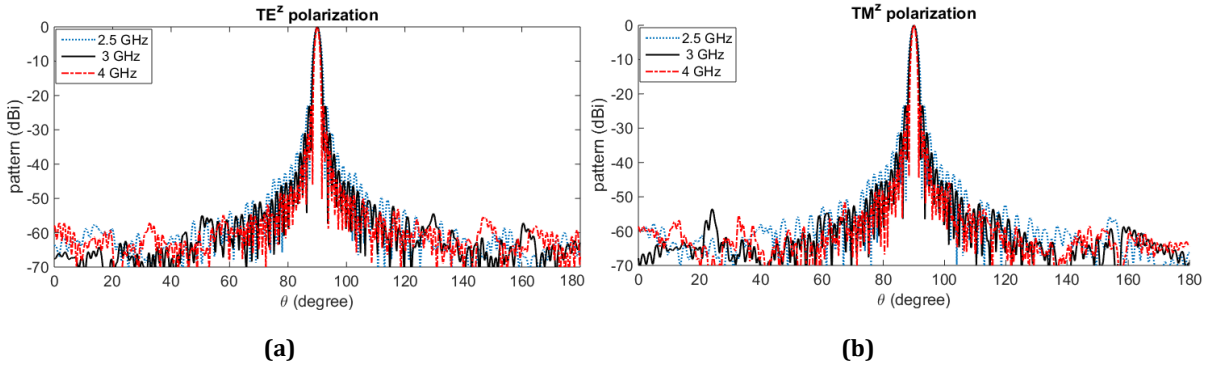


Fig. 9. Frequency variation of radiation pattern in azimuth plane, (a) TE^z polarization, (b) TM^z polarization

during the optimization procedure. The application of physical optics and uniform theory of diffraction properly copes with this challenge.

Although the antenna synthesis has been performed at single frequency 3 GHz, the synthesized reflector for the center frequency shows good characteristics in other frequencies of S-band. The far-field radiation patterns in the elevation and azimuth planes at 2.5, 3 and 4 GHz are shown in Fig. 8 and Fig. 9 respectively. The length of the antenna is considered 4 m along the z-axis. The computed gain, \bar{E}_{csc^2} and \bar{E}_{sll} of the reflector at those frequencies are presented in Table III. As observed, the reflector retains its low side lobe level at lower, mid and upper frequencies of the band.

A final note should be mentioned about the optimization algorithm. Particle Swarm Optimization (PSO) [17] and Invasive Weed Optimization (IWO) [6]–[9] are other evolutionary algorithms that have been successfully used in the literature for reflector shaping. In our design, GA performed well and resulted in good pattern characteristics in terms of pattern shape (cosecant-squared) and achieved side-lobe level. However, PSO and IWO can also be used and may provide faster convergence and better pattern characteristics.

IV. CONCLUSION

A dual polarized cylindrical offset reflector antenna has been designed in this paper to achieve cosecant-squared radiation pattern in S-band. In the design procedure the cross section of the reflector has been modeled with a polynomial function of degree 6. The coefficients of the polynomial have been initially selected as those of a cylindrical parabolic reflector. These coefficients are then optimized by genetic algorithm to achieve cosecant-squared radiation pattern in angular span of 3° - 50° . The side lobe level of -25 dB has also been implemented in the cost function for other elevation angles.

Utilizing the physical optics and uniform theory of diffraction has enhanced the computational efficiency of the optimization. The large size of the antenna with respect to wavelength justifies the application of these two asymptotic methods for calculating the radiation pattern. This is a vital point particularly in the optimization process, since the induced current density (and consequently the radiation pattern) can be efficiently calculated for a large population size in each iteration of the optimization.

The numerical results show that desired characteristics of the radiation pattern can be achieved with good accuracy for both TE and TM polarizations. The calculated radiation pattern deviates about or less than 0.8 dB on average from the ideal cosecant-squared pattern. Furthermore, the side lobe level is kept below -25 dB out of the angular range of main beam. To ensure the validity of the results, the radiation pattern of the optimized antenna has been calculated with CST software as well as the method of moments, which agree quite well with the PO-UTD results. Therefore, the procedure presented in this paper can be used to accurately and efficiently design the cylindrical reflector for achieving the cosecant-squared radiation pattern.

REFERENCES

- [1] M. I. Skolnik, *Introduction to Radar Systems*, 3 ed., New York, NY: McGraw Hill, 2001.
- [2] J. R. Bergmann, F. J. V. Hasselmann, L. C. P. Pereira and M. G. Castello Branco, "Reflector antenna configurations for radio base stations in cellular communications," *IEEE-APS Conference on Antennas and Propagation for Wireless Communications (Cat. No.98EX184)*, Waltham, MA, 1998, pp. 61-64.
- [3] M. Koubeissi, L. Freytag, C. Decroze and T. Monediere, "Design of a Cosecant-Squared Pattern Antenna Fed by a New Butler Matrix Topology for Base Station at 42 GHz," *IEEE Antennas and Wireless Propagation Letters*, vol. 7, pp. 354-357, 2008.
- [4] N. Herscovici, "A simple cosec² microstrip array: the shovel-microstrip array," *IEEE Antennas and Propagation Magazine*, vol. 35, no. 4, pp. 42-44, Aug. 1993.
- [5] A. Haddadi, A. Ghorbani and J. Rashed-Mohassel, "Cosecant-squared pattern synthesis using a weighted alternating reverse projection method," *IET Microwaves, Antennas & Propagation*, vol. 5, no. 15, pp. 1789-1795, Dec. 2011.

- [6] A. Dastranj, H. Abiri, and A. Mallahzadeh, "Two-dimensional synthesis and optimization of a broadband shaped beam reflector antenna using IWO and PSO algorithms," *RF and Microwave Computer-Aided Engineering*, vol. 25, no. 2, pp. 129-140, June 2014.
- [7] A. Dastranj, H. Abiri, and A. Mallahzadeh, "Design of a Broadband Cosecant Squared Pattern Reflector Antenna Using IWO Algorithm," *IEEE Transactions on Antennas and Propagation*, vol. 61, no. 7, pp. 3895-3900, July 2013.
- [8] A. Foudazi, and A. R. Mallahzadeh, "Pattern synthesis for multi-feed reflector antenna using invasive weed optimization algorithm," *IET Microwaves, Antennas & Propagation*, vol. 6, no. 14, pp. 1583-1589, Nov. 2012.
- [9] A. A. Dastranj, H. Abiri, and A. R. Mallahzadeh, "Cosecant-squared pattern synthesis method for broadband-shaped reflector antennas," *IET Microwaves, Antennas & Propagation*, vol. 8, no. 5, pp. 328-336, April 2014.
- [10] O. M. Bucci, A. Capozzoli, and G. D'Elia, "An effective power synthesis technique for shaped, double-reflector multifeed antennas," *Progress in Electromagnetics Research*, vol. 39, pp. 93-123, 2003.
- [11] F. S. Adana, O. Gutierrez, I. Gonzalez, M. F. Catedra, L. Lozano, *Practical Applications of Asymptotic Techniques in Electromagnetics*, Norwood, MA: Artech House, 2011.
- [12] D. Dah-Weihand, Y. Rahmat Samii, "A generalized diffraction synthesis technique for high performance reflector antennas," *IEEE Transactions on Antennas and Propagation*, vol. 43, no. 1, pp. 27-40, Jan 1995.
- [13] C. A. Balanis, *Advanced Engineering Electromagnetics*, 2nd ed., Hoboken, NJ: Wiley, 2012.
- [14] C. A. Balanis, *Antenna Theory: Analysis and Design*, 4th ed., Hoboken, NJ: Wiley, 2016.
- [15] A. S. Glassner, *An Introduction to Ray Tracing*, London, UK: Academic Press, 1989.
- [16] D. E. Goldberg, *Genetic Algorithms in Search, Optimization, and Machine Learning*, Reading, MA: Addison-Wesley, 1989.
- [17] J. Robinson and Y. Rahmat-Samii, "Particle swarm optimization in electromagnetics," *IEEE Transactions on Antennas and Propagation*, vol. 52, no.2, pp. 397-407, Feb. 2004.